

# Impact of Surface and Volume Modification of Nickel Superalloys IN-713C and MAR-247 on High Temperature Creep Resistance

M. Cieśla\*, F. Binczyk, M. Mańka

Chair of Materials Technology, Silesian University of Technology, Krasinskiego 8, 40-019 Katowice, Poland

\*Corresponding author. E-mail address: marek.ciesla@polsl.pl

Received 06.07.2012; accepted in revised form 03.09.2012

## Abstract

Impact of surface and volume modification and double filtration during pouring the moulds on basic mechanical properties and creep resistance of nickel superalloys IN-713C and MAR-247 in conditions of accelerated creep of castings made of post-production scrap of these alloys is evaluated in this paper. The conditions of initiation and propagation of cracks in the specimens were analysed with consideration of stereological properties of material macro- and microstructure. It has been proven that in the conditions of high-temperature creep at 980°C and at stress  $\sigma = 150$  MPa, creep resistance of superalloy MAR-247 is more than 10 times higher than the creep resistance of IN-713C alloy. In case of IN-713C alloy, the creep resistance negligibly depends on macrograin sizes. But, the macrograin size considerably affects the time to failure of specimens made of alloy MAR-247. Creep resistance of specimens made of coarse grain material was 20% higher than the resistance of fine grain materials.

**Keywords:** Nickel superalloys, Macrostructure, Modification, Mechanical properties, Creep

## 1. Introduction

Creep-resisting Ni-based alloys are primary materials used for manufacturing of critical elements of aircraft jet engines, mainly for rotating and guide vanes. [1,2]. Material of vanes should guarantee their reliable operation for the period from few hundreds to few thousands hours at the temperature reaching in some instances 1100°C [1,3]. Time varying force fields caused by unsteady flow of waste gas and aerodynamic interactions between jet engine elements, which cause vane destruction owing to material fatigue and creep, are one of the most frequently occurring phenomena at high temperature. [4,5]. Moreover, intensity of corrosion processes, changes in material structure and

deterioration of its mechanical strength increase adverse effects of high temperature on vane life-time.

In order to fully benefit from the use of creep-resisting materials, the knowledge of creep mechanisms dominating in specific operating conditions is required. In case of nickel superalloys for casting, the evaluation of impact of superalloy chemistry, conditions of casting and parameters of modification process determining morphological properties of macro- and microstructure on creep resistance results obtained in short-term creep tests is particularly important. These tests deliver information of material behaviour in extreme operating conditions. In many instances, such evaluation may considerably depart from the results obtained in long-term creep tests. [6-9]. In

many cases, creep mechanisms in the long- and short-term tests are different. Generally, dislocation mechanism of deformation prevails in short-term creep tests, while slip along grain boundaries, even when considering diffusion creep in accordance with Nabarro-Herring-Coble model, is usually the most common in long-term creep tests [7,10].

Advanced grades of nickel and cobalt alloys form the basic group of castings which meets the quality requirements set at the most critical components of aircraft jet engines exposed to maximum loads such like turbine disks, compressor vanes, HP turbine vanes, and others. Following superalloys are suitable for the foregoing applications: INCONEL-100, INCONEL-738, RENE-77, RENE-80, MAR-M257 and MAR-M509. They are precipitation-hardened alloys, which produce specific macrostructure composed of equal-axial, frozen and columnar grains during solidification. Such alloy structure may support crack initiation and propagation, which may cause dangerous aircraft engine failures [13,14]. Moreover, as the manufacturing experience shows, the impurities, which are present at the beginning of melting feedstock ingots tend to appear also in the castings of aircraft engine components (e.g. in vane castings). These impurities during casting and in case of insufficient filtration migrate to liquid alloy while melting, and finally to the castings. One of the methods leading to improved structure and properties of castings made of nickel alloys is surface [12,13] and volume [14-18] modification.

Impact of surface and volume modification and double filtration during pouring the moulds on basic mechanical properties and creep resistance of nickel superalloys IN-713C and MAR-247 in conditions of accelerated creep of castings made of post-production scrap of these alloys is evaluated in this paper. Processes of destruction occurred to the most loaded jet engine components in extreme operating conditions were simulated in the tests. Conditions of initiation and propagation of cracks in specimens were analysed with consideration of stereological properties of material macro- and microstructure. The results of laboratory tests enable preliminary assessment of suitability of various technologies of nickel superalloy modifications for specific applications in aircraft jet engines.

## 2. Material and test method

For testing of basic mechanical strength and creep resistance, four groups of threaded specimens of sizes (M12,  $d_o = 6.0$  mm,  $l_o = 32$  mm) were prepared. The specimens for the tests of mechanical strength and macro- & microstructure observations were taken from the castings for which the scrap remaining after production of nickel superalloys IN-713C and MAR-247 was the input material. The castings were produced in following four casting experiments:

- I-1. Melt IN-713C (B), (a form of blue, blue filter),
- I-2. Melt IN-713C (W), (a form of white, blue filter),
- II-1. Melt MAR-247 (B), (a form of blue, blue filter),
- II-2. Melt MAR-247 (W), (a form of white, blue filter).

Ingots were molten in crucible made of  $Al_2O_3$ , and subsequently cast in Vacuum Induction Melting Furnace – type: IS 5/III manufactured by Leybold-Heraeus. In the experiment I-2 and II-2, macrostructure of material was formed in conditions of volume modification treatment only, while in the experiment I-1 and II-1 – in

combined modification treatment (i.e. surface and volume modification).

Combined surface and volume modification required using of so called “blue mould” (with a modifying coat of  $CoAl_2O_4$ ) and providing additional strainer core with cobalt aluminate in pouring basin. Additional effect of this solution was double alloy filtration.

Mechanical properties of alloys IN-713C and MAR-247 at room temperature and at 800°C were determined in static tensile test carried out in testing machine MTS-810. Specimens were inductively heated, and accurate strain amount was measured with use of extensometer.

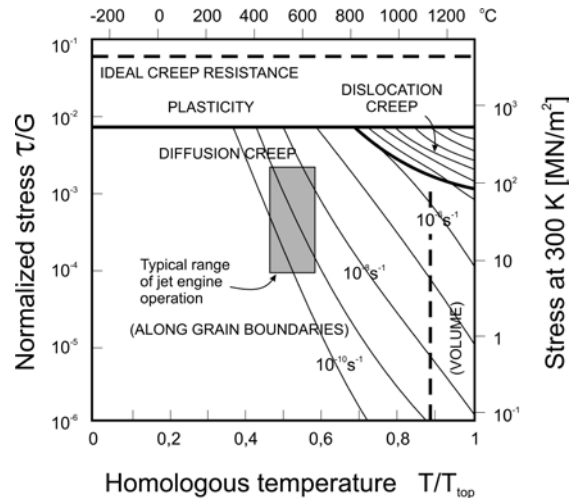


Fig. 1. Map of deformation mechanism of Mar-M200 alloy, grain size 100  $\mu$ m [11]

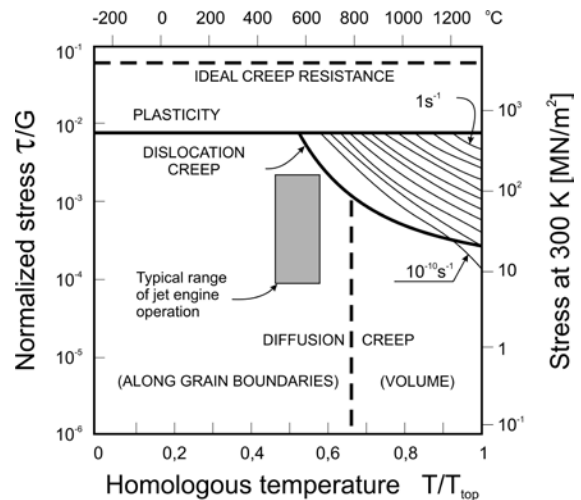


Fig. 2. Map of deformation mechanism of Mar-M200 alloy, grain size 10  $\mu$ m [11]

Creep tests were performed in Walter-Bai AG LFMZ-30kN testing machine. The tests were conducted at the temperature of 982°C and axial load causing the stress  $\sigma_0 = 157$  MPa in cross-section area of specimens. Creep tests were carried out in simulated conditions corresponding to extreme operating conditions of vanes of aircraft jet engines. In the adopted test conditions, normalized stress value  $\tau/G$  amounted to approx.  $10^{-3}$  at homologous temperature

$T/T_{top} \approx 0.71 \div 0.73$ , what, basing upon analysis of deformation mechanism map for this group of alloys (Figures 1 and 2), [11] gives a reason to assume that the plastic strain in creep process of tested superalloys occurs mainly as a result of diffusion creep caused by atomic diffusion along grain boundaries. In such conditions, pursuant to Coble model, creep rate is described by the following formula [19]:

$$\dot{\epsilon}_s = 50\sigma D_{gz} b^4 / kTd^3 \quad (1)$$

where:  $\sigma$  – stress,  $D_{gz}$  – coefficient of diffusion along grain boundaries,  $b$  – Burgers vector,  $k$  – Boltzmann constant,  $T$  – absolute temperature,  $d$  – grain diameter.

It is to note that in the conditions of conducted creep tests, material deformation caused by volume diffusion (Nabarro-Herring's model) and diffusion along the grain boundaries may occur concurrently, and contribution of each of these processes to the deformation depends on temperature, stress, grain size, and structure of grain boundaries. The

diffusion along the grain boundaries precedes the occurrence of volume diffusion because the activation energy of the former one amounts to 0.4-0.7 of the activation energy of the latter one [19]. The mentioned models of diffusion creep (Nabarro-Herring-Coble) describe the diffusion-controlled creep with some approximation, because they do not consider dominating dislocation mechanism of creep [20].

### 3. The results of investigations and discussion of results

Images of macrostructures of tested castings and of specimens subjected to creep process are given in Table 1. Preparations for microscope observations were etched in Marble agent. Table 1 specifies also stereological parameters of grains formed in modification processes of superalloys IN-713C and MAR-247.

Table 1.  
Images of macrostructure and stereological parameters of macrograins observed in superalloys IN-713C and MAR-247

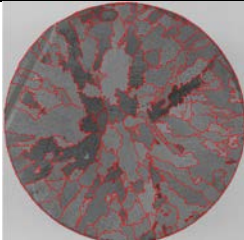
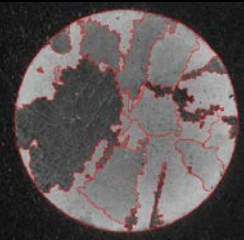
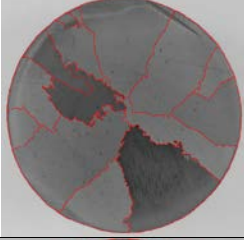
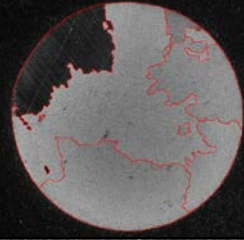
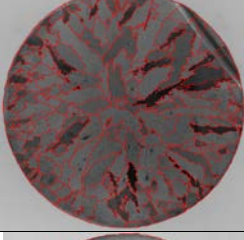
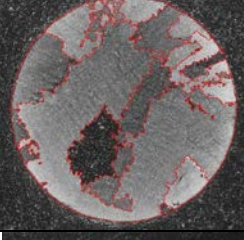
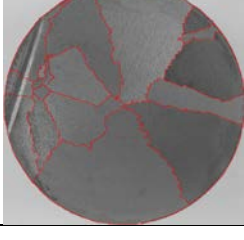
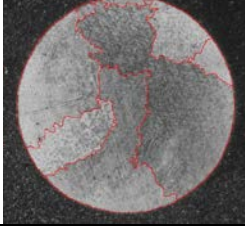
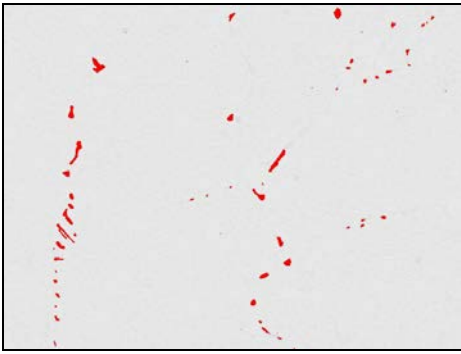
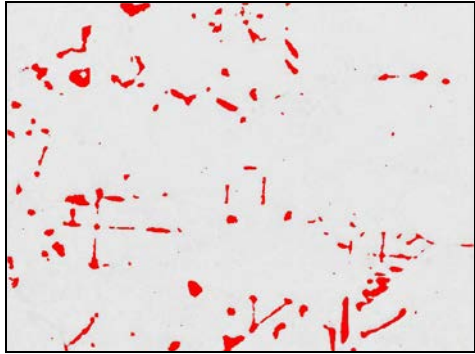
Heat	Evaluation of macrostructure			
	Ingot, $d_0 \cong 21$ mm	Macrostructure parameters	Specimen for creep test $d_0 \cong 6$ mm	Macrostructure parameters
I-1 (B) IN-713C		0.388 - number of grains per 1 mm <sup>2</sup> 2.58 mm <sup>2</sup> - average grain surface, 0.415 - shape coefficient		33 - number of grains, 1.3 - number of grains per 1 mm <sup>2</sup> 0.76 mm <sup>2</sup> - average grain surface 0.42 - shape coefficient
I-2 (W) IN-713C		0.042 - number of grains per 1 mm <sup>2</sup> 23.8 mm <sup>2</sup> - average grain surface, 0.387 - shape coefficient		14 - number of grains 0.52 - number of grains per 1 mm <sup>2</sup> 1.93 mm <sup>2</sup> - average grain surface, 0.58 - shape coefficient
II-1 (B) MAR-247		0.668 - number of grains per 1 mm <sup>2</sup> 1.51 mm <sup>2</sup> - average grain surface,		45 - number of grains, 1.7 - number of grains per 1 mm <sup>2</sup> 0.57 mm <sup>2</sup> - average grain surface, 0.56 - shape coefficient
II-2 (W) MAR-247		0.045 - number of grains per 1 mm <sup>2</sup> 22.03 mm <sup>2</sup> - average grain surface,		7 - number of grains, 0.1 - number of grains per 1 mm <sup>2</sup> 3.55 mm <sup>2</sup> - average grain surface, 0.31 - shape coefficient

Table 2.

Examples of images of precipitated carbides in microstructure of nickel superalloys IN-713C and MAR-247

IN-713C, heat I-1 (B)	MAR-247, heat II-1 (B)
	
Carbide content in surface area $A_A$	
$A_A = 0.74 \%$	$A_A = 2.12 \%$

In Table 2, characteristic structures of carbides precipitated from the specimens subjected to high temperature creep tests are given as an example. Basic parameters of macrostructure were evaluated with use of Met-Ilo software.

Metallographic observations demonstrated that the effect of only volume modification was formation of coarse grain structure in superalloys, while the combined simultaneous volume and surface modification resulted in occurrence of fine grain structure (Table 1). The performed casting processes confirmed also an important impact of casting temperature on stereological properties of macrostructure. The lower the casting temperature is the finer grains are produced by modifying effect. Investigations of carbide precipitations, which are important from the point of view of tested alloys strength and creep resistance, confirmed higher content of carbides in surface area ( $A_A$ ) of superalloy MAR-247 (Table 2). Primary carbides (mainly in form of “Chinese characters”) occurred in this case in grain boundary area.

Taking into account the impact of high temperature and stress on stability of nickel superalloy structure, metallographic observations of these materials were carried out after completion of creep tests. It was found out that in both alloys: IN-713C and MAR-247, morphology of

the phase  $\gamma'$  changed as a result of coalescence from the initial cuboid form to the irregular, coagulated form after creep process (Figures 3, 4). At the same time,  $\gamma''$  – the areas between carbide phase precipitation  $\gamma'$  (“matrix corridors”) increased. In these “corridors”, precipitation of very fine dispersed phase  $\gamma'$  was found after creep process (Figures 3, 4).

Basic mechanical properties ( $R_m$ ,  $R_{0.2}$ ,  $A_5$ ) of nickel superalloys at room temperature and at 800°C are specified in Tables 3 and 4. At both temperatures, MAR-247 alloy, after the same modification processes, had higher strength properties than IN-713C alloy. In case of IN-713C alloy, volume and surface modification caused increase of yield point and tensile strength by approx. 7.5% and approx. 3-15%, respectively as a result of grain size reduction for both, room temperature and 800°C.

Contrary to the foregoing, the strength values of MAR-247 alloy after volume and surface modification were lower as a result of macrograin size reduction (Tables 1, 3, 4). This effect was particularly noticeable at 800°C. Moreover, both superalloys of coarse grain structure had tensile strength ( $R_m$ ) at 800°C higher by 4-13% than their respective tensile strength determined at the room temperature.

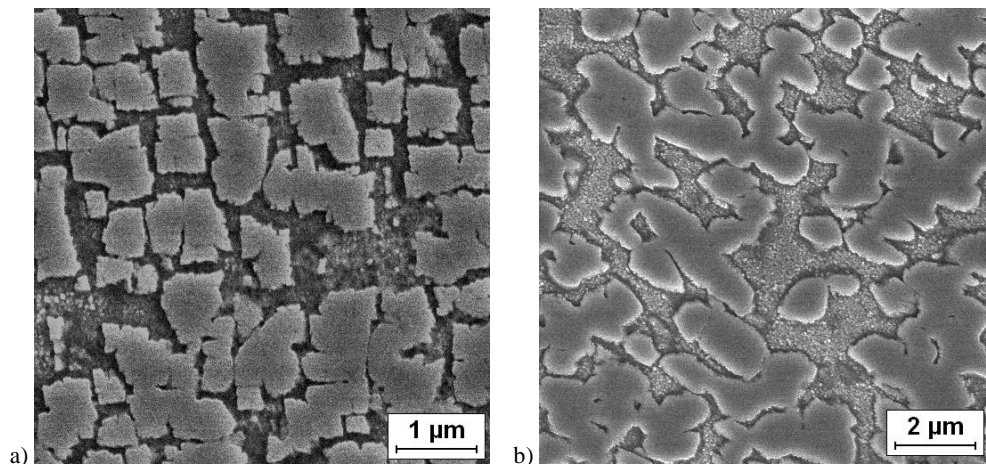


Fig. 3. Morphology of phase  $\gamma'$  in alloy IN-713C (I-2 casting). Initial conditions – a, conditions as after creep process,  $t_c = 26.7 \text{ h}$  – b



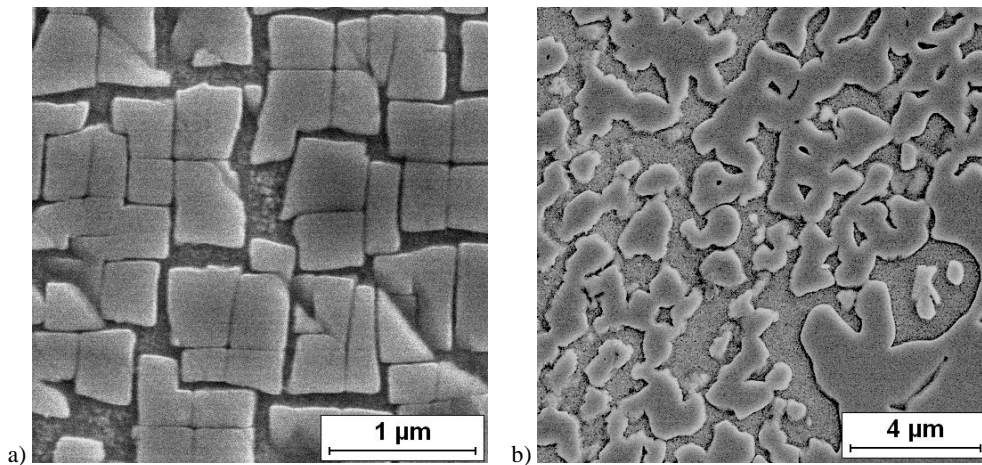


Fig. 4. Morphology of phase  $\gamma'$  in alloy MAR-247 (II-2 casting). Initial conditions – a, conditions as after creep process,  $t_z = 317.4$  h – b

Table 3.

Mechanical properties of nickel superalloys: IN-713C and MAR-247 at room temperature

Heat	Material	Tensile strength $R_m$ , MPa	Yield point $R_{0.2}$ , MPa	Unit elongation $A_5$ , %	Young's modulus $E$ , MPa
I-1 (B)	IN-713	923	785	7.3	$2.15 \cdot 10^5$
I-2 (W)		804	736	5.3	
II-1 (B)	MAR-247	964	808	6.9	$2.18 \cdot 10^5$
II-2 (W)		944	848	7.2	

Table 4.

Mechanical properties of nickel superalloys: IN-713C and MAR-247 at 800°C

Heat	Material	Tensile strength $R_m$ , MPa	Yield point $R_{0.2}$ , MPa	Unit elongation $A_5$ , %	Young's modulus $E$ , MPa
I-1 (B)	IN-713	933	763		$1.58 \cdot 10^5$
I-2 (W)		907	706		
II-1 (B)	MAR-247	939	734		$1.47 \cdot 10^5$
II-2 (W)		980	786		

Creep characteristics of superalloys IN-713C and MAR-247 are shown on Figure 5. In Tables 5 and 6 stereological parameters of tested alloy microstructure such like time to specimen failure  $t_z$  and steady state creep rate  $V_u$  referenced to the creep characteristics are given. These values are of considerable importance for identification of factors which determine material high temperature creep resistance. Analysis of the results obtained demonstrates that the high temperature creep resistance  $t_z$  of MAR-247 superalloy is more than 10 time higher than in case of IN-713C alloy. In case of IN-713C superalloy, this resistance negligibly depends on macrograin size and amounts to  $t_z = 26.7$  h for specimen of coarse grain structure and 25.4 h for specimen of fine grain structure obtained after volume and surface modification (Table 5). On the other hand, the macrograin size of the specimen made of MAR247 alloy affected considerably the time to specimen failure in high temperature creep test. Creep resistance of specimens made of coarse grain material was 20% higher than the resistance of fine grain material.

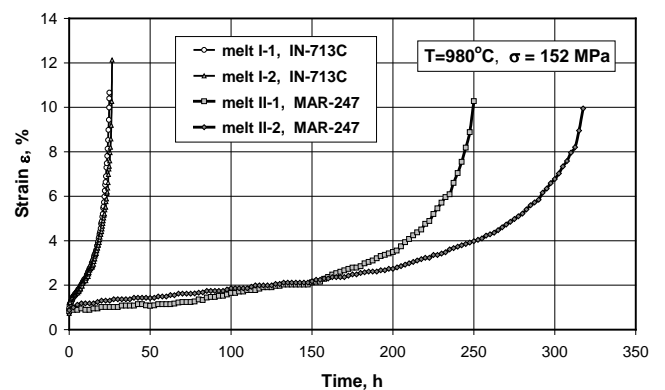


Fig. 5. Creep characteristics of nickel superalloys: IN-713C and MAR-247

Table 5.

Creep resistance and selected stereological parameters of microstructure of nickel superalloys IN-713C and MAR-247

Heat	Material	Resistance, time to specimen failure $t_z$ , h	Carbide content in surface area $A_A$ , %	Average surface of flat grain cross section $A$ , $\text{mm}^2$	Number of grains on specimen cross-section $N$
I-1 (B)	IN-713C	25.35	0.74	2.58	33
I-2 (W)		26.7	0.92	23.8	14
II-1 (B)	MAR-247	250.25	2.12	1.51	45
II-2 (W)		317.38	1.45	22.03	7

Table 6.

Creep resistance and selected stereological parameters of microstructure of nickel super alloys IN-713C and MAR-247

Heat	Material	Resistance, time to specimen failure $t_z$ , h	Steady-state creep rate $V_u$ , %/h	Ratio of carbide content in surface area and number of grains $A_A/N$ , %
I-1 (B)	IN-713C	25.35	0.13	0.022
I-2 (W)		26.7	0.11	0.066
II-1 (B)	MAR-247	250.25	0.0086	0.047
II-2 (W)		317.38	0.0080	0.21

As the data comprised in Table 5 show, creep resistance of tested materials strictly depends on carbide content in surface area  $A_A$  found in their microstructure. This influence is good described by the implemented parameter  $A_A/N$ , (ratio of carbide content in surface area and number of grains in specimen, Table 6). For any of the tested superalloys, the higher the value of this parameter was, the higher the creep resistance  $t_z$  and the lower the steady state creep  $V_u$  were (Table. 6). It explains good the impact of carbide content on inhibition of crack propagation process by, among others, inhibiting slip along grain boundaries. Content of carbide in surface area of the specimens made of MAR-247 alloy was much higher than in specimens made of IN-713C alloy because of higher carbon content in the former one (0.12% [w/w] vs. 0.07% C [w/w]). Value of  $A_A/N$  ratio was also bigger (Table 6). Higher creep resistance of alloy MAR-247 may also pertain to high content in the microstructure of the phase  $\gamma'$ , content of hafnium (approx. 1.3%), which supports strengthening the phase  $\gamma'$ , content of boron (0.015% [w/w]) which strengthens grain boundaries and supports reduction of amount of carbides of unfavourable morphology at the grain boundaries [21]. Higher creep resistance of MAR-247 alloy than the resistance of IN-713 alloy was also a result of very high stability of the phase  $\gamma'$  (resistance to high growth and coagulation, Figures 3 and 4) observed in conditions of conducted creep tests. Alloy additives dissolved in the matrix of superalloy MAR-247 (Co, W, Mo, Cr, Ta, Hf), by strengthening of the phase  $\gamma$  and mitigation of impact on diffusion-type volume processes at high temperature, contributed also to obtaining creep resistance higher than in case of IN-713C alloy.

Observations of microstructure of specimens made of both superalloys: IN-713 and MAR-247 after creep process demonstrated that a thin layer of complex oxides comprising Cr, Al and Ti was formed on specimen surface in creep conditions. On the other hand, reduced content of elements forming oxide phase in sub-surface area caused dissolution of the phase  $\gamma'$  in alloy matrix (Figure 6). In subsequent stages of creep process, crack initiation process was running (Figure 6a) in the area of lower mechanical properties, consequence of which was

propagation of cracks along macrograin boundaries (Figure 6b) and finally, the specimen failure.

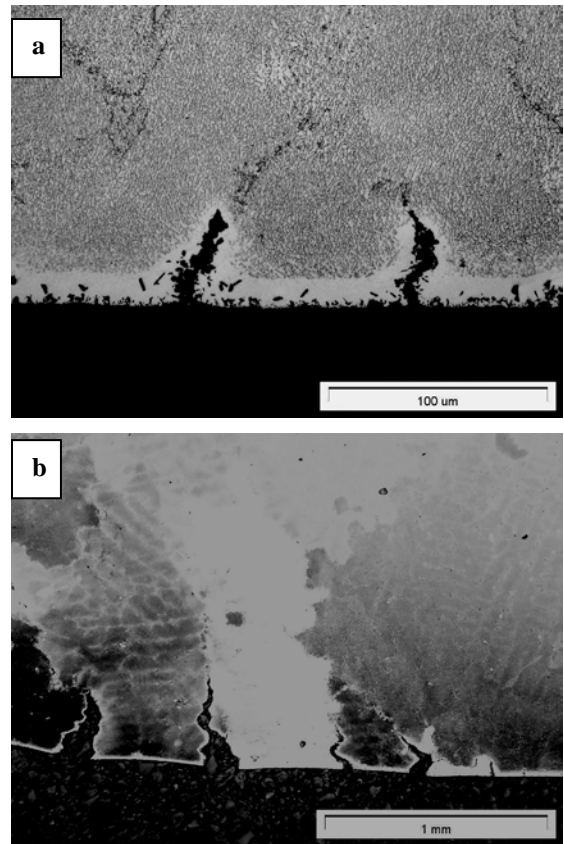


Fig. 6. Microstructure of IN-713C alloy after creep test. Effect of crack occurrence in surface area of the specimen taken from the casting I-2 – (a), crack propagation along macrograin boundaries observed in the specimen taken from the casting I-1 – (b)

The conducted observations of microstructure of specimens made of MAR-247 alloy demonstrated also inhibition of crack propagation on numerous precipitations of plastic eutectics  $\gamma\text{-}\gamma'$  (Figure 7) and on precipitations of primary carbides within the grain boundaries. Similar impact of carbides was observed in coarse grain specimens made of IN-713C alloy (Figure 8).

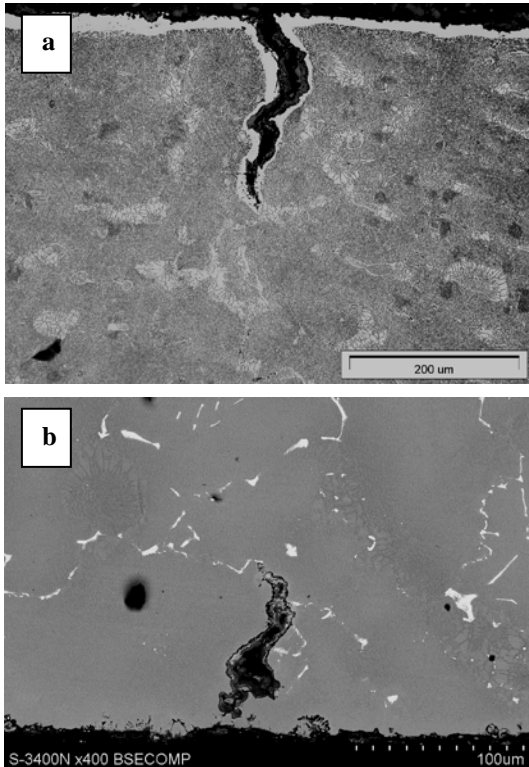


Fig. 7. Microstructure of MAR-247 alloy after creep test (specimens taken from the casting II-2). Effect of crack propagation inhibition on eutectics precipitations – (a), and on precipitations of primary carbides within the grain boundaries – (b)

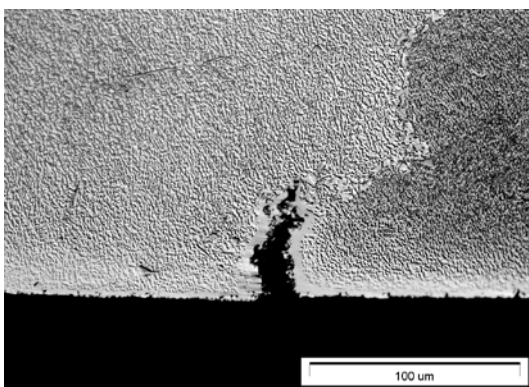


Fig. 8. Microstructure of IN-713C superalloy after creep test. Effect of crack propagation inhibition on precipitations of primary carbides within the grain boundaries

## 4. Conclusions

When analysing the deformation processes occurring in the test conditions of superalloys MAR-247 i IN-713C, the assumption may be made that in the given test conditions ( $t = 980^{\circ}\text{C}$ ,  $\sigma = 150 \text{ MPa}$ ) dislocation mechanism of deformation determined the creep resistance of the alloys. Slip along grain boundaries controlled crack initiation and propagation processes. In this case the factor, which determines the creep resistance of a given superalloy was a ratio of carbide content in surface area and number of grains on specimen cross-section area ( $A_A/N$ ). The higher the ratio was the higher the creep resistance of the material was.

Diffusion creep along the grain boundaries, which determines the steady-state creep rate  $V_u$ , was less noticeable in the conducted creep tests (Table 6). Nevertheless, the tested superalloys of fine grain microstructure showed higher  $V_u$  values (by few percent).

## References

- [1] Y. Tamarin, Protective coatings for turbine blades, ASM International, The Materials Information Society, Materials Park, Ohio (2002).
- [2] A.K. Koul, V.R. Parameswaran, J-P. Immarrigeon, W. Wallace, Advances in High Temperature Structural Materials and Protective Coatings, A Publication from National Research Council of Canada, Ottawa (1994).
- [3] Y. Tamarin, Protective Coatings for Turbine Blades, ASM International The Materials Information Society, Materials Park, Ohio (2002).
- [4] Seon-gab Kim, Young-ha Hwang, Tae-gu Kim, Chang-min Shu, Failure analysis of J85 engine turbine blades, Engineering Failure Analysis, vol. 15 (2008) 394-400.
- [5] Haijun Tang, Dashu Cao, Hongyu Yao, Mingli Xie, Ruichun Duan, Fretting fatigue failure of an aero engine turbine blade, Engineering Failure Analysis, vol. 16 (2009) 2004-2008.
- [6] A. Strang, E. Lang, R. Pichoir, Practical implications of the use of aluminide coatings for the corrosion protection of superalloys in gas turbines, Materials Substitution and Recycling, AGARD Conference Proceedings SMP 356 (1983).
- [7] A. Strang, High Temperature Properties of Coated Superalloys, Behaviour of High Temperature Alloys in Aggressive Environments, The Metals Society, London, UK (1980) 595-611.
- [8] M. Cieřla, Durability of ŹS6U nickel superalloy with aluminide protective layer in thermal and mechanical load conditions, Monograph, Editor: Wydawnictwo Pol. Śl. (in polish) (2009).
- [9] J. Okrajni, M. Cieřla, L. Swadźba, High-Temperature Low-Cycle Fatigue and Creep Behaviour of Nickel-Based Superalloys with Heat-Resistant Coatings. Fatigue and Fracture of Materials and Engineering Structures, vol. 21 (1998) 947-954.
- [10] R. Castillo R., A.K. Koul, J-P. Immarrigeon, The Effects of Service Exposure on the Creep Properties of Cast IN-738LC Subjected to Low Stress High Temperature Creep

- Conditions, Superalloys 88, S. Reichman, D.N. Duhl, G.Maurer, S. Antolovich, C. Lund, Eds., The Metallurgical Society (1988).
- [11] H.J. Frost, M.F. Ashby, Deformation-Mechanism Maps. The plasticity and creep of metals and ceramics, Oxford, Pergamon press (1982) 166.
- [12] M. Zielińska, J. Sieniawski, M. Poreba, Microstructure and mechanical properties of high temperature creep resisting superalloy Rene 77 modified  $\text{CoAl}_2\text{O}_4$ , Archives of Materials Science and Engineering, vol. 28, issue 10 (2007) 629-632.
- [13] M. Zielińska, J. Sieniawski, M. Wierzińska, Effect of modification on microstructure and mechanical properties of cobalt casting superalloy, Archives of Metallurgy and Materials, vol. 53, issue 3 (2008) 887-893.
- [14] F. Binczyk, J. Śleziona, Effect of modification on the mechanical properties of IN-713C alloy, Archives of Foundry Engineering, vol. 10, issue 1 (2010) 195-198.
- [15] F. Binczyk, J. Śleziona, Mechanical properties and creep resistance behaviour of IN-713C alloy castings, Archives of Foundry Engineering, vol. 10, issue 4 (2010) 9-13.
- [16] F. Binczyk, J. Śleziona, P. Gradoń, Modification of the macrostructure of nickel superalloys with cobalt nanoparticles, Composites, no. 1 (2011) 49-55.
- [17] F. Binczyk, J. Śleziona, P. Gradoń, Ceramic filters for bulk inoculation of nickel alloy castings, Archives of Foundry Engineering, vol. 11, special issue 3 (2011) 29-33.
- [18] F. Binczyk, J. Śleziona, The ATD thermal analysis of selected nickel superalloys, Archives of Foundry Engineering, vol. 10, issue 2 (2010) 13-19.
- [19] J. Wyrzykowski, E. Pleszakow, J. Sieniawski, Deformation and cracking of metals (in polish), WNT Warszawa (1999).
- [20] M.Ł. Bernsztejn, W.A. Zajmowski, Structure and mechanical properties of metals (in polish), WNT Warszawa (1973).
- [21] C.T. Sims, W.C. Hagel, N.S. Stoloff, Superalloys II High temperature materials for aerospace and industrial power, Ed. John Wiley & Sons Inc (1987).